Am J Transl Res 2026;18(9):8298-8313
www.ajtr.org /ISSN:1943-8141/AJTR0174782

Original Article

Downregulation of exosomal miR-432-5p promotes keratinocyte proliferation and inflammation in pediatric atopic dermatitis via the E2F2/STAT1 axis

Chenchen Si*, Wei Wu*, Minhua Shao, Jie Pu, Zhewen Zhou, Feini Xu, Ting Yang

Department of Dermatology, Affiliated Children's Hospital of Jiangnan University, Wuxi 214023, Jiangsu, China.
**Equal contributors and co-first authors.*

Received June 16, 2026; Accepted September 1, 2026; Epub September 15, 2026; Published September 30, 2026

Abstract: Objectives: To investigate whether serum exosomes from children with severe atopic dermatitis (AD) affect keratinocyte function and to explore the underlying molecular mechanisms. Methods: Exosomal fractions were obtained from sera of severe AD patients (AD-Exos) and healthy counterparts (NH-Exos), and were characterized using transmission electron microscopy and nano-flow cytometry. Cultured HaCaT cells were exposed to these exosomes or transfected with miR-432-5p mimic/inhibitor. RT-qPCR was employed to quantify inflammatory cytokine mRNAs, while CCK-8 assays, flow cytometry and immunoblotting were used to evaluate proliferation, apoptosis and pathway proteins. A dual-luciferase reporter system and RNA pull-down experiments confirmed the direct mRNA target of miR-432-5p. Receiver operating characteristic (ROC) curves were constructed to appraise the biomarker potential of exosomal miR-432-5p. Results: AD-Exos promoted HaCaT cell proliferation and upregulated IL-1β, IL-31, and IL-33 compared to NH-Exos. miRNA sequencing and RT-qPCR revealed that miR-432-5p was significantly downregulated in AD-Exos. Functional experiments showed that miR-432-5p mimic suppressed proliferation, enhanced apoptosis, and reduced inflammatory cytokine release, while miR-432-5p inhibition produced opposite effects, mimicking the action of AD-Exos. Mechanistically, miR-432-5p directly targeted E2F2, and E2F2 overexpression reversed the anti-inflammatory and pro-apoptotic effects of the miR-432-5p mimic. Furthermore, miR-432-5p inhibited STAT1 phosphorylation via E2F2 downregulation. ROC analysis indicated that exosomal miR-432-5p can distinguish AD patients from healthy controls (AUC = 0.87). Conclusions: Downregulation of miR-432-5p in AD-derived exosomes relieves its suppression on E2F2, thereby promoting HaCaT cell proliferation and inflammatory responses. Restoring miR-432-5p levels may represent a potential therapeutic strategy for severe pediatric AD.

Keywords: Atopic dermatitis, exosome, HaCaT cell, miR-432-5p, inflammation

Introduction

Atopic dermatitis (AD) is a common, chronically relapsing inflammatory dermatosis that presents with intense pruritus and a protracted course. It is reported to be one of the most burdensome skin diseases worldwide [1]. Recent data from a study show that the prevalence of AD in children aged 1-7 years in urban areas is 12.94%, and for children aged 1-12 months, it is as high as 30.48% [2]. Children with AD may subsequently develop allergic diseases such as rhinitis and asthma, forming a process known as the "atopic march", a process that can have serious clinical consequences [3-5]. The etiology of AD is multifactorial, which poses challenges for current clinical management [6]. Therefore, elucidating the exact pathogenic mechanisms of AD is both necessary and of great interest.

Currently, researchers believe that keratinocytes are the fundamental cells of the skin barrier and are also involved in the progression of AD. Abnormal differentiation of these cells leads to structural damage in the stratum corneum, a reduction in the amount of filaggrin and ceramides, weakened skin barrier protection, and thus increased permeability to external allergens and pathogens [7, 8]. A previous study [9] has shown that exosomes in the blood can exert both beneficial and detrimental

https://doi.org/10.62347/FVMI8873

Table 1. Basic information of the included population

Characteristic	Total (N = 46)	Group1 (AD, n = 23)	Group 2 (NH, n = 23)	*P* value
Age, years, mean ± SD	7.28 ± 3.20	7.26 ± 3.14	7.30 ± 3.41	> 0.999
Sex, n (%)				> 0.999
Male	30 (65.2)	15 (65.2)	15 (65.2)	
Female	16 (34.8)	8 (34.8)	8 (34.8)	
Age at onset, years, median (IQR)		1 (0.5-2.0)	NA	
Disease duration, years, median (IQR)		6 (4.0-8.0)	NA	
Atopic family history, n (%)	20 (43.5)	20 (87.0)	0	< 0.001
IGA score, n (%)				
3	10 (21.7)	10 (43.5)	0 (0)	
4	13 (28.3)	13 (56.5)	0 (0)	
Comorbidities and medications, n (%)				-
Allergic rhinitis	17 (37.0)	17 (73.9)	0 (0)	
Asthma	3 (6.5)	3 (13.0)	0 (0)	
Allergic conjunctivitis	12 (26.1)	12 (52.2)	0 (0)	
Food allergy	2 (4.3)	2 (8.7)	0 (0)	

effects on keratinocytes. These vesicles are efficient carriers, delivering proteins, lipids and non-coding RNAs to specific cells to alter their behavior [10]. MicroRNAs (miRNAs) are the main cargo components of exosomes and are responsible for their functional effects [11]. Studies have shown that exosomal miRNAs affect skin photoaging [12]. Therefore, exosomal miRNAs are now recognized as key regulatory molecules.

Many studies have explored plasma miRNAs as diagnostic markers or functional regulators in AD [13-15], but circulating miRNAs are relatively unstable and easily degraded. Exosomal miRNAs are more stable due to the protective function of the exosomal phospholipid membrane, and are frequently employed as diagnostic indicators in many diseases [16-18]. Recently, few studies have investigated exosomal miRNAs in atopic dermatitis [19, 20]. Therefore, this study is the first to identify exosomal miRNA signatures in children with severe AD, determine whether serum-extracted exosomes from AD patients (AD-Exos) carry cellular signals that affect the phenotype of HaCaT cells, clarify the basic molecular mechanisms of AD, and offer new ideas for clinical treatment.

Methods

Research population and ethical approval

Twenty-three children (aged 2-18 years) with severe AD and 23 age- and sex-matched healthy controls were recruited from the Department of Dermatology, Affiliated Children's Hospital of Jiangnan University (2024-2025). Three cases in the AD group and three cases in the control group were subjected to RNA sequencing. Each patient met the Williams criteria for AD and had an SCORAD score of 50 or more. Healthy controls were specifically required to have no personal history of allergic diseases (including allergic rhinitis, asthma, food allergy, or drug allergy), no first-degree family history of atopy, and no active or previous skin disorders. None of the subjects had any inborn diseases or autoimmune diseases. Written informed consent was obtained from the guardians of all pediatric participants. The study protocol was approved by the hospital ethics committee (WXCH2023-09-057). Demographic and clinical characteristics are summarized in **Table 1**.

Cell culture and cell transfection

HaCaT cells (Shangen Biosciences, Wuhan, China) were cultured in DMEM supplemented with 10% non-exosome fetal bovine serum and 1% penicillin-streptomycin at 37°C in 5% CO_2. Serum-derived exosomes were normalized by protein concentration and applied at the indicated doses. miR-432-5p mimics, inhibitors, and negative controls were synthesized by RiboBio (Guangzhou, China). Lipofectamine™ 2000 (Thermo Fisher, MA, USA) was used for transfection according to the supplier's protocol. Cells at ~50% confluency in six-well

plates were incubated with transfection complexes for 48 h. E2F2-overexpressing plasmids (pcDNA3.1(+), with NheI-EcoRI restriction sites) were purchased from Genecfps (Jiangsu, China). A short interfering RNA (siRNA) (gctactgctacctactacaca) specifically targeting E2F2 mRNA was prepared by Genecfps (Jiangsu, China). Co-transfection of miR-432-5p mimic and OE-E2F2 was performed under the same conditions using Lipofectamine™ 2000 Reagent.

Exosome isolation and labeling

Peripheral blood (10 mL) was collected in EDTA-free tubes, centrifuged at 3000×g for 15 min at 4°C to obtain serum. Exosomes were pelleted using a commercial extraction reagent (KeyGEN, Jiangsu, China) at a 4:1 (serum-to-reagent) ratio, incubated at 4°C for 2 h with gentle shaking, and then centrifuged at 12,000×g for 20 min at 4°C. Morphology and size distribution of exosomes were examined by transmission electron microscopy (Philips, WA, USA) and nano-flow cytometry.

Nano-flow cytometry

Nano-flow cytometry (NanoFCM, serial No.: FNAN30E20071514) was performed using a 488 nm laser using V2.0 software. Samples were diluted in particle-free PBS to prevent coincidence of signals. The scattering intensity was calibrated with 68-155 nm fluorescent beads. Particles within the 30-200 nm range were selected to avoid aggregates and background noise. Particle size distribution, concentration and fluorescence intensity were measured independently three times. Quantitative data and single-particle distributions were processed using the instrument's software.

Uptake of exosomes by HaCaT cells

Purified exosomes were labelled with PKH26 (4 μL, 1:250 dilution in Diluent C; Beyotime, Shanghai) for 5 min at room temperature, then washed twice by ultracentrifugation (100,000×g, 70 min, 4°C). Labelled exosomes (50 μL in PBS) were added to HaCaT cells for 12 h. After fixation in 4% paraformaldehyde, permeabilization with 0.5% Triton X-100, and staining with phalloidin-AF488 (1:500, 30 min) and DAPI (1:20,000, 5 min), cells were visualized by fluorescence microscopy.

MiRNA sequencing

Total RNA was extracted from serum-derived exosomes using TRIzol reagent (Takara, Tokyo, Japan). RNA quality and quantity were assessed with a NanoDrop ND-1000 (Thermo Scientific, MA, USA). MiRNA sequencing was performed as previously described [21]. A small RNA library was constructed, and raw data were obtained through Illumina sequencing. Reads were aligned to the Ensembl GRCh38 genome; rRNA and tRNA reads were filtered using the Rfam database. miRDeep2 quantified small RNAs, and differentially expressed miRNAs were defined by FDR-adjusted $P < 0.05$ and $|\log_2 FC| \geq 1$.

Real-time qPCR (RT-qPCR)

RNA from exosomes or cells was reverse-transcribed with a PrimeScript™ RT kit (Takara, Tokyo, Japan) qPCR was performed using TB Green (Takara, Tokyo, Japan) on a real-time system. U6 and GAPDH served as internal controls, and relative expression was calculated by the $2^{-\Delta\Delta CT}$ method. Primer sequences are listed in **Table 2**.

Western blot

Protein extracts from exosomes or cell lysates were separated on 10% SDS-polyacrylamide gels, electro-transferred onto PVDF membranes (Roche), blocked with 5% skim milk, and incubated overnight at 4°C with primary antibodies against CD9, E2F2, β-actin (Origene), CD63, TSG101, Calnexin, STAT1, phospho-STAT1 (P-STAT1), and p53 (Proteintech). After washes with TBST, membranes were incubated with HRP-conjugated secondary antibodies (Servicebio) for 1 hour at room temperature. Bands were visualized by enhanced chemiluminescence.

Immunofluorescence staining

HaCaT cells on coverslips were transfected for 48 h, fixed with 4% paraformaldehyde, permeabilized with 0.2% Triton X-100, and blocked with 5% BSA, then incubated with primary antibodies against E2F2 (Thermo) and p-STAT1 (Cell Signaling Technology) overnight at 4°C. Following washes, Alexa Fluor 488- and 594-labelled secondary antibodies were applied for 1 hour in the dark. Nuclei were stained with

Table 2. The RT-qPCR gene sequence in the text

	Sequence	species	Primer uses
Forward	AAGCTCATTTCCTGGTATGACAA	human	GAPDH
Reverse	CTTACTCCTTGGAGGCCATGT	human	GAPDH
Forward	CCGACGTAGGTAGTTTCATGTT	human	hsa-miR-196a-5p
Reverse	GTGCAGGGTCCGAGGTATTC	human	
RT	GTTGGCTCTGGTGCAGGGTCCGAGGTATTCGCACCAGAGCCAACCCCAAC	human	
Forward	CTCGCTTCGGCAGCACA	human	hsa-U6
Reverse	AACGCTTCACGAATTTGCGT	human	
RT	GTTGGCTCTGGTGCAGGGTCCGAGGTATTCGCACCAGAGCCAACAAAATATGG	human	
Forward	GCGGCGGTCTTGGAGTAGGTCATT	human	miR-432-5p
Reverse	ATCCAGTGCAGGGTCCGAGG	human	
RT	GTCGTATCCAGTGCAGGGTCCGAGGTATTCGCACTGGATACGACCCACCC	human	
Forward	CCTTGGAGGCTACTGACAGC	human	E2F2
Reverse	CCACAGGTAGTCGTCCTGGT	human	E2F2
Forward	CGACGTCTGTGCTCTTTCTG	human	IL-31
Reverse	AGCATCTTCGAGAGGGACTG	human	IL-31
Forward	ACTATGAGTCTCAACACCCCTCAA	human	IL-33
Reverse	TACCATCAACACCGTCACCTGAT	human	IL-33
Forward	ACAGATGAAGTGCTCCTTCCAG	human	IL-1β
Reverse	TTGCTGTAGTGGTGGTCGGA	human	IL-1β

DAPI. Confocal images (Zeiss LSM 800) were captured, and mean fluorescence intensities were calculated with ImageJ.

Proliferation and apoptosis assays

For CCK-8, cells (1×10^4/well) in 96-well plates were treated for 48 h, then 10 μL CCK-8 solution (Solarbio, Beijing, China) was added and incubated for 2 h; absorbance at 450 nm was recorded. Ki-67 staining was performed using a PE-conjugated antibody (BD Pharmingen, NJ, USA) followed by flow cytometry. Apoptosis was measured with an FITC-Annexin V kit (Thermo Scientific, MA, USA) and flow cytometry.

Luciferase reporter assay

The wild-type (WT) or mutated (MUT) 3'UTR of E2F2 was cloned into pmirGLO. HaCaT cells were co-transfected with the reporter plasmid and miR-432-5p mimic or NC using Lipofectamine 2000. After 48 h, luciferase activity was measured with the Dual-Luciferase® Reporter Assay System (Promega, USA) on a GloMax® Discover plate reader.

Biotin-labeled miRNA pull-down assay

HaCaT cells were transfected with biotin-tagged miR-432-5p mimic (bio-miR-432-5p) or bio-NC. After 48 h, lysates were incubated with streptavidin-coated magnetic beads at 4°C for 12 h. Beads were washed, and bound RNA was extracted; E2F2 mRNA enrichment was quantified by RT-qPCR.

Statistical analysis

All experiments were performed at least thrice. Data were expressed as mean ± SEM. Group comparisons were performed using Student's t-test or the Mann-Whitney U test for two groups, and one-way ANOVA followed by Tukey's pos-hoc test for multiple groups. *p*-value < 0.05 was considered statistically significant. GraphPad Prism 9.0 was employed for all analyses.

Results

Extraction and analysis of exosomes from serum of young children with serious AD

Exosomes were isolated from the serum of children with severe AD and from healthy control children (NH). Transmission electron microscopy revealed typical cup-shaped or spherical vesicles with lipid bilayer membranes (**Figure 1A**). Nano-flow cytometry (NanoFCM) was performed to measure the size distribution and concentration of AD-derived small extracellular

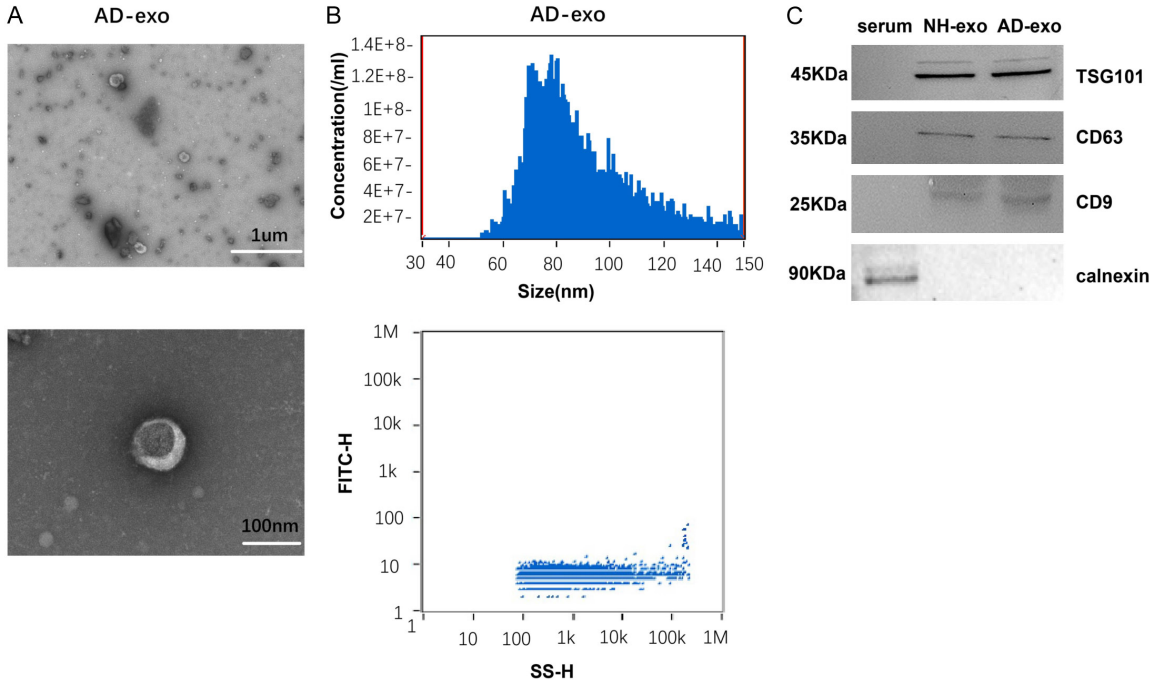


Figure 1. Characterization of exosomes isolated from the serum of AD patients and healthy controls (NH). A. Transmission electron microscopy images showing the morphology of isolated exosomes. Scale bars: 100 nm/1 μm. B. NanoFCM analysis of particle size distribution. The size distribution histogram shows a bimodal distribution with a mean diameter of 89.4 nm. The scatter plot of side scatter height (SS-H) versus FITC fluorescence height (FITC-H) confirms the high purity of the exosome preparation with minimal background noise and no detectable fluorescent contaminants. C. Western blot analysis of exosomal markers CD63, CD9, and TSG101, and the negative control calnexin, in AD-Exos and NH-Exos. AD, atopic dermatitis; NH, healthy control.

vesicles. The mean particle size was 89.4 nm, which falls within the typical exosome size range (30-150 nm), with a peak particle concentration of 1.2×10^8 particles/mL (**Figure 1B**), indicating a high yield of isolated vesicles. The corresponding scatter plot of side scatter height (SS-H) versus FITC fluorescence height (FITC-H) demonstrated a relatively homogeneous particle population, with minimal background noise and no detectable large aggregates or fluorescent contaminants. Finally, exosomes from both AD and NH serum groups expressed the exosomal markers CD63, CD9, and TSG101, while Calnexin (a negative control) was undetectable (**Figure 1C**). These results collectively confirmed that exosomes were successfully isolated and characterized.

Effect of AD-exosomes on the proliferation and inflammatory response in HaCaT cells

To investigate the effect of AD-Exos on HaCaT cells, PKH-26-labeled AD-Exos were added to the cell culture, and their internalization was observed by fluorescence microscopy. As shown in **Figure 2A**, labeled exosomes were taken up by HaCaT cells and accumulated mainly in the perinuclear regions. To establish a standardized working concentration for comparative analyses, HaCaT cells were initially treated with varying concentrations of NH-Exos (0, 20, 40, and 60 μg/mL). CCK-8 assays demonstrated that a concentration of 40 μg/mL NH-Exos produced a robust and reproducible cellular response (**Figure 2B**). To enable a direct functional comparison between NH-Exos and AD-Exos at an equivalent dosage, 40 μg/mL was selected as the standardized intervention concentration for subsequent experiments. Notably, HaCaT cells treated with 40 μg/mL AD-Exos showed significantly higher cell survival than those exposed to the same concentration of NH-Exos (**Figure 2C**). RT-qPCR showed that IL-1β, IL-31, and IL-33 mRNA levels were markedly higher in the AD-Exo group (**Figure 2D-F**). Collectively, these results suggest that AD-Exos are taken up by HaCaT cells and promote cell proliferation and pro-inflammatory cytokine production.

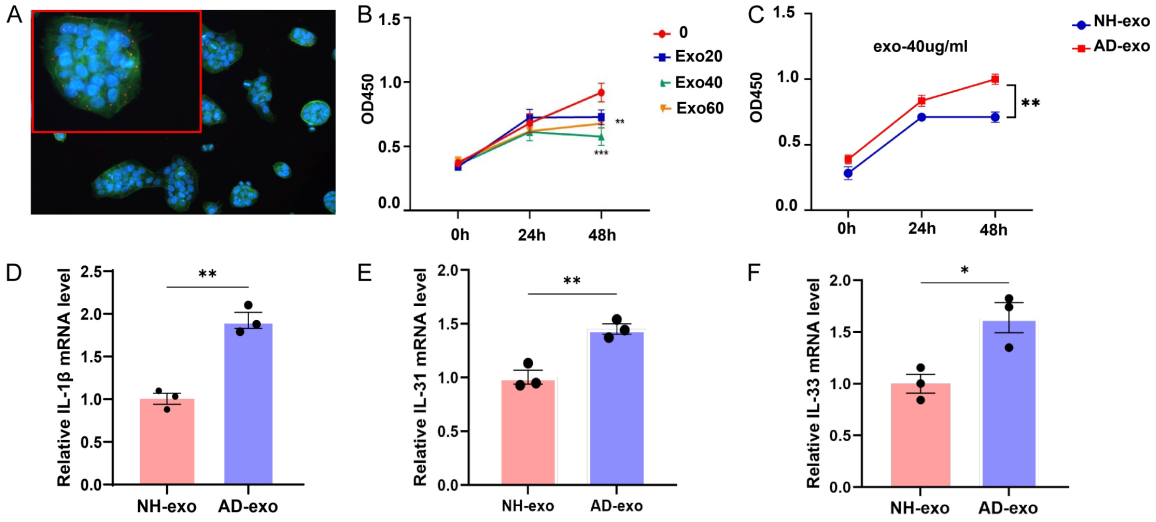


Figure 2. AD-Exos promote proliferation and inflammatory responses in HaCaT cells. A. PKH-26-labelled (red fluorescent) AD-Exos have been taken up by HaCaT cells. Scale bar: 50 μm, ×200. B, C. CCK-8 assays measured changes in HaCaT cell viability after exosome treatment. D-F. RT-qPCR was used to quantify the amounts of IL-1β, IL-31, and IL-33 in HaCaT cells after being treated with 40 μg/mL of AD AD-Exos or NH-Exos. $^{*}P < 0.05$, $^{**}P < 0.01$, $^{***}P < 0.001$. A total of nine experiments were carried out in triplicate.

MiR-432-5p is downregulated in AD-Exos and selected as the relevant molecule

Serum exosomal miRNAs were analyzed using samples from three severe AD patients and three healthy individuals. Volcano plots identified seven miRNAs that were downregulated in the AD-Exo group (FDR-adjusted $P < 0.05$ and $|\log2FC| \geq 1$; **Figure 3A**, **3B**): hsa-miR-196a-5p, hsa-miR-4492, hsa-miR-4508, hsa-miR-7704, hsa-miR-432-5p, hsa-miR-4516, and hsa-let-7c-5p. Bioinformatics analysis showed that these dysregulated miRNAs are enriched in multiple signaling pathways, including p53, MAPK, PI3K/AKT, and cGMP-PKG, which are related to inflammatory immune responses or cell growth and differentiation (**Figure 3C**, **3D**). RT-qPCR validation confirmed that both miR-196a-5p and miR-432-5p were significantly reduced in AD-Exos (**Figure 3E**, **3F**). Based on the determination of exosomal miR-432-5p levels in 46 pediatric subjects and ROC curve generation, an AUC of 0.87 (95% CI: 0.74-0.99) was obtained, with a cut-off value of 0.75 (**Figure 3G**). Thus, exosomal miR-432-5p can serve as an early indicator to distinguish severe AD patients from healthy individuals.

MiR-432-5p ameliorates dysfunction in HaCaT cells

To study how miR-432-5p is involved in the physiology of HaCaT cells, overexpression of miR-432-5p via mimic transfection significantly reduced the transcripts of IL-1β, IL-31 and IL-33 (**Figure 4A-C**), decreased P-STAT1 protein levels and increased p53 levels (**Figure 4D**), dampened proliferation (CCK-8 and Ki-67, **Figure 4E**, **4F**), and promoted apoptosis (**Figure 4G**). In contrast, the miR-432-5p inhibitor produced the opposite pattern, phenotypically mimicking AD-Exos. Hence, loss of miR-432-5p recapitulates the effects of AD-Exos.

MiR-432-5p inhibitor can reproduce AD-Exo function in HaCaT cells

To determine whether inhibition of miR-432-5p could replicate the effects in AD-Exos-treated HaCaT cells, a miR-432 inhibitor was added to the cells to suppress the expression of miR-432-5p. RT-qPCR showed that the levels of IL-1β, IL-31 and IL-33 were significantly higher in the miR-432-inhibitor + NH-Exos group compared to the inhibitor NC + NH-Exos group (**Figure 5A-C**). Western blotting showed that the miR-432-inhibitor + NH-Exos group effectively reproduced the increase in p-STAT1 and decrease in p53 induced by AD-Exos (**Figure 5D**). In addition, the miR-432-inhibitor + NH-Exos group showed significantly higher proliferation (**Figure 5E**, **5F**) and lower apoptosis (**Figure 5G**) compared to the inhibitor NC + NH-Exos group. Importantly, direct statistical comparisons of the miR-432-inhibitor + NH-Exos group with the AD-Exos group revealed

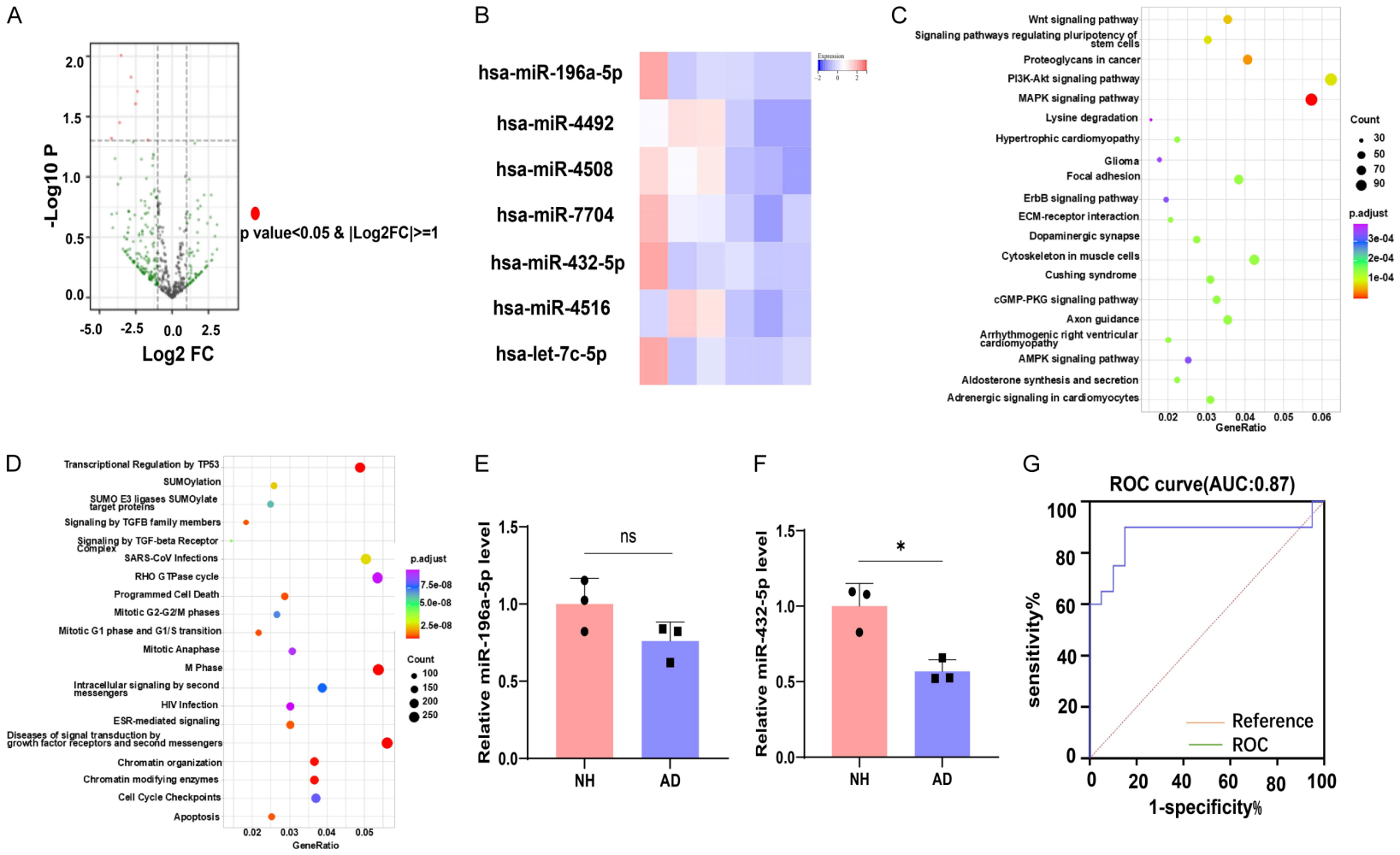


Figure 3. miR-432-5p shows reduced abundance in AD-Exos and has been identified as the main mediator. A. Volcano plot of miRNA sequencing data. B. A heat map shows the seven different exosomal miRNAs specifically. C, D. KEGG pathway and GO term analyses revealed the enrichment of these dysregulated miRNAs in multiple signaling pathways. E, F. RT-qPCR was used to quantify the amounts of miR-432-5p and miR-196-5p. G. ROC curve assessed the diagnostic performance of exo-miR-432-5p in severe AD. $^{*}P < 0.05$.

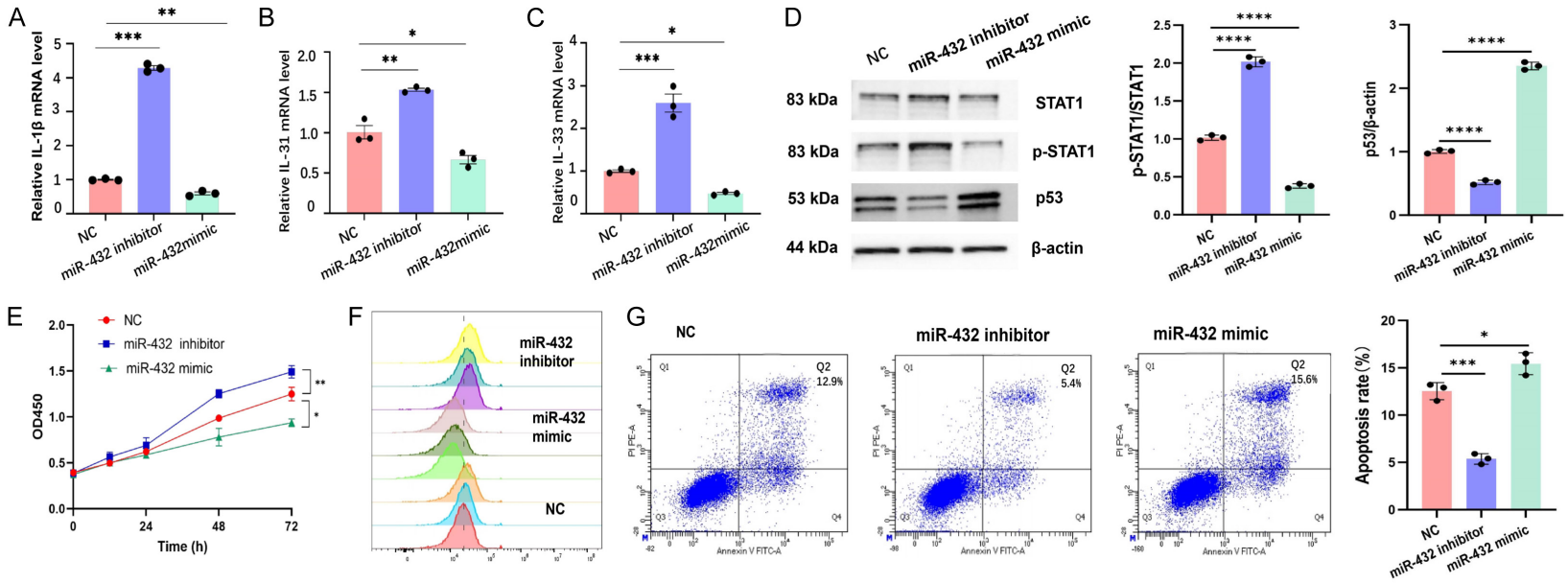


Figure 4. miR-432-5p modulates proliferation, apoptosis, and inflammation in HaCaT cells. A-C. RT-qPCR analysis of IL-1β, IL-31, and IL-33 mRNA levels in HaCaT cells transfected with miR-432-5p mimic, inhibitor, or negative control (NC). D. Western blot analysis of STAT1, P-STAT1, and p53 protein levels after transfection. E. CCK-8 assay measuring cell viability after transfection. F. Flow cytometry analysis of Ki67 staining intensity. G. Flow cytometry analysis of apoptosis using Annexin V-FITC staining. Data are presented as mean ± SEM. $^{*}P < 0.05$, $^{**}P < 0.01$, $^{***}P < 0.001$, $^{****}P < 0.0001$. All experiments were performed in triplicate.

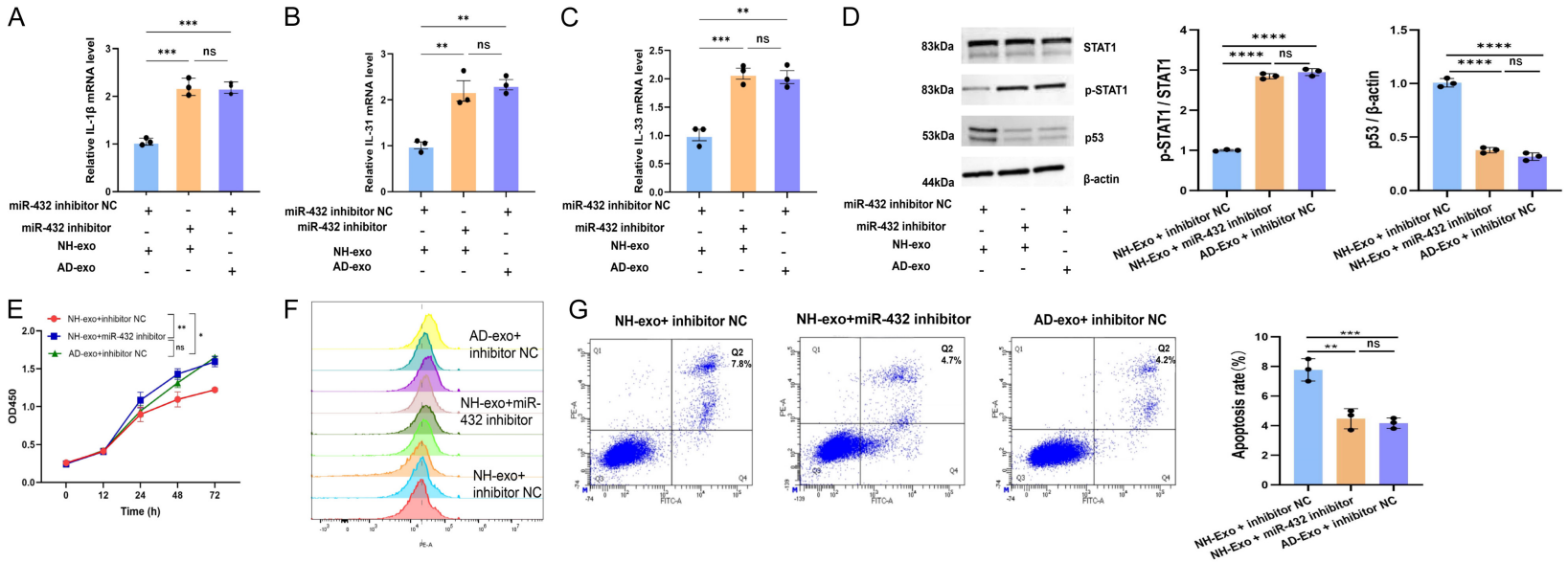


Figure 5. miR-432-5p inhibitor reproduces AD-Exos effects in HaCaT cells. A-C. RT-qPCR evaluation of the concentration of IL-1β, IL-31 and IL-33 in different cohorts to show the effect of miR-432 inhibitor on the secretion of pro-inflammatory factors from HaCaT cells stimulated by AD-Exos or NH-Exos. D. Expression levels of STAT1, P-STAT1 and p53 are shown to indicate the effect of miR-432-5p inhibitor on HaCaT cells exposed to AD-Exos or NH-Exos. E, F. Cell proliferation rates of HaCaT cells after various treatments were determined by CCK8 and Ki67 immunofluorescence staining. G. Determine the percentage of apoptotic HaCaT cells after various treatments by flow cytometry. Data are in the form of mean ± SEM. $^{*}P < 0.05$, $^{**}P < 0.01$, $^{***}P < 0.001$, $^{****}P < 0.0001$. A total of 9 replicates were used for the three treatments.

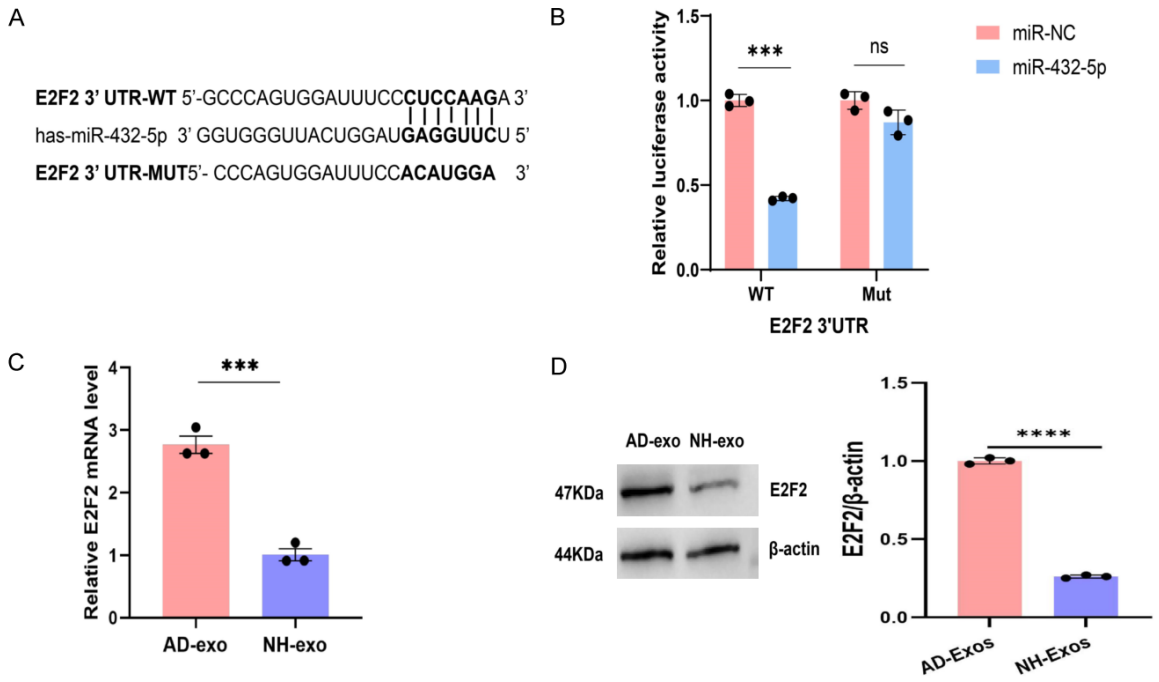


Figure 6. E2F2 is a direct target of miR-432-5p. (A) The exact arrangement of miR-432-5p in the 3'-UTR of E2F2 mRNA is shown below. (B) A dual-luciferase assay confirms that miR-432-5p binds to the 3'-UTR of E2F2. (C) and (D) miR-432-5p regulates both the mRNA expression (C) and protein levels (D) of E2F2. The mean ± SEM of the results is shown in a bar chart. $^{*}P < 0.05$, $^{**}P < 0.01$, $^{***}P < 0.001$, $^{****}P < 0.0001$. Three sets of replicates were set up for all the experiments.

no significant differences in the expression levels of IL-1β, IL-31, IL-33, p-STAT1/STAT1 ratio, p53 protein levels, cell proliferation rates, or apoptosis percentages. These results confirm that the loss of miR-432-5p is a major mediator of AD-Exo-induced changes.

E2F2 is a downstream target of miR-432-5p

TargetScan predicted a conserved miR-432-5p binding site within the E2F2 3'UTR (**Figure 6A**). Dual-luciferase assays demonstrated that the miR-432-5p mimic significantly diminished luciferase activity driven by the wild-type E2F2 3'UTR, whereas the mutant construct abolished this effect (**Figure 6B**). In HaCaT cells, AD-Exos markedly upregulated E2F2 mRNA and protein compared with NH-Exos (**Figure 6C**, **6D**), in line with the reduced miR-432-5p levels.

MiR-432-5p directly binds to E2F2 mRNA and reduces the translation efficiency of this mRNA, as shown in the pull-down and immunofluorescence experiments

To obtain direct biochemical evidence of a link between miR-432-5p and E2F2 mRNA, biotin-labelled miRNA pull-down assays were performed. As shown in **Figure 7A**, E2F2 mRNA was significantly enriched in the bio-miR-432-5p pull-down samples. Immunofluorescence analysis also showed that miR-432-5p mimic significantly reduced the fluorescence intensity of E2F2 and p-STAT1 proteins in HaCaT cells, while miR-432-5p inhibitor increased their fluorescence (**Figure 7B**, **7C**). Based on these results, miR-432-5p directly inhibits E2F2 expression through post-transcriptional mechanism and consequently reduces STAT1 activation.

Overexpression of E2F2 reversed dysfunction in miR-432-5p-treated HaCaT cells

Co-transfection of the miR-432-5p mimic with an E2F2-expressing plasmid reversed the suppressive effects of the mimic on IL-1β, IL-31 and IL-33 (**Figure 8A-C**), restored p-STAT1 and p53 levels (**Figure 8D**), abolished the anti-proliferative effect (**Figure 8E**, **8F**), and counteracted the pro-apoptotic action (**Figure 8G**). Thus, E2F2 serves as a critical effector through which miR-432-5p regulates keratinocyte function.

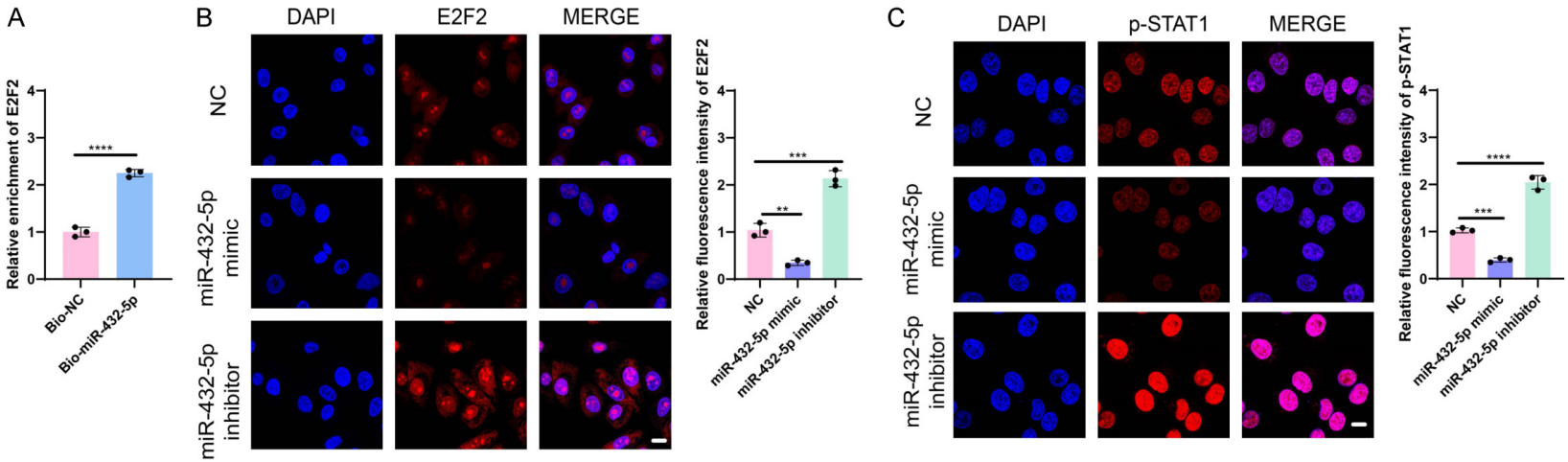


Figure 7. miR-432-5p directly binds to E2F2 mRNA and downregulates E2F2 and p-STAT1 expression. A. RNA pull-down assay showing enrichment of E2F2 mRNA in HaCaT cells transfected with biotin-labeled miR-432-5p mimic (bio-miR-432-5p) compared with biotin-labeled negative control (bio-NC). B, C. Immunofluorescence staining and fluorescence intensity analysis of E2F2 and P-STAT1 in HaCaT cells after miR-432-5p mimic, inhibitor or NC transfection. A Scale Bar of 10 μm. The results are presented as mean ± SEM, and $^{*}P < 0.05$, $^{**}P < 0.01$, $^{***}P < 0.001$, $^{****}P < 0.0001$. A total of three replicates were carried out for all groups.

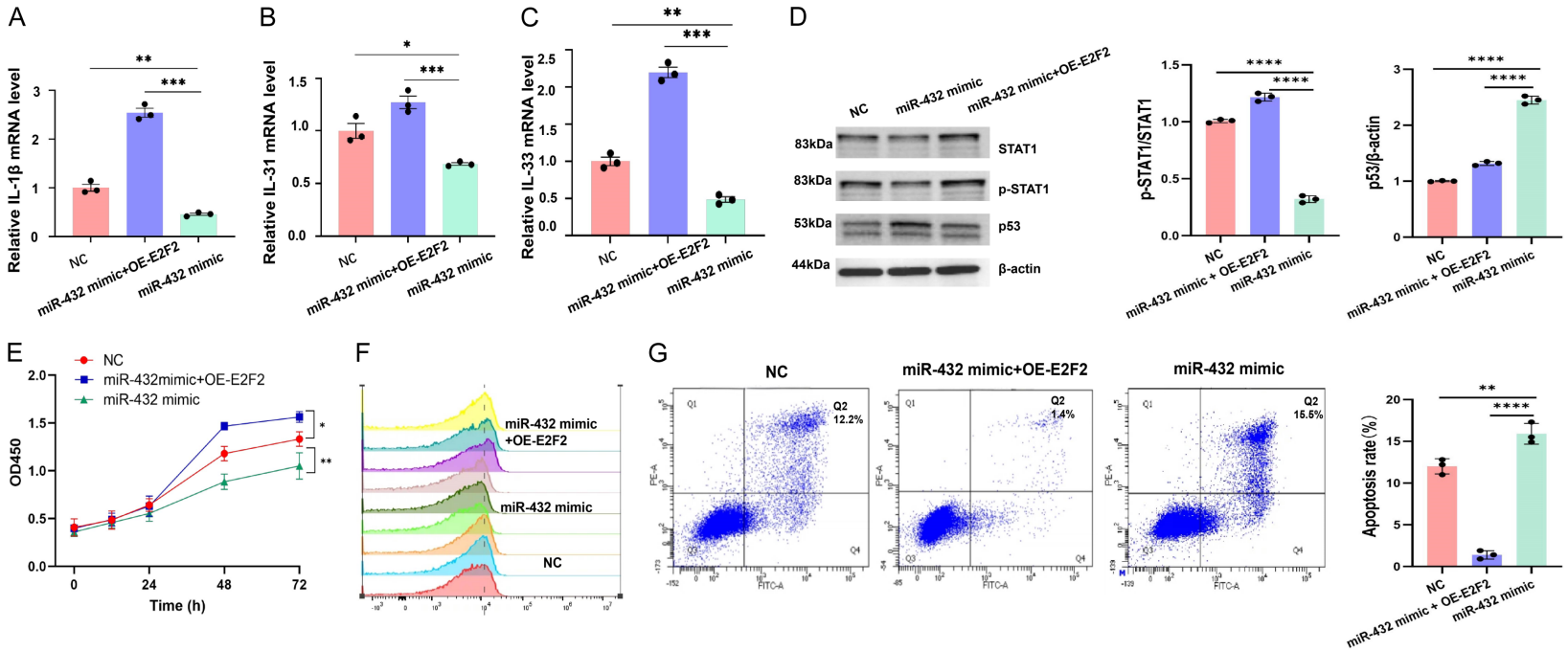


Figure 8. Overexpression of E2F2 reverses the effects of miR-432-5p mimic in HaCaT cells. A-C. RT-qPCR for IL-1β, IL-31, and IL-33 mRNA. D. Western blotting for STAT1, P-STAT1, and p53. E, F. CCK-8 assay and Ki67 immunofluorescence for cell proliferation. G. Flow cytometry for apoptosis. Results are presented as mean ± SEM, and $^{*}P < 0.05$, $^{**}P < 0.01$, $^{***}P < 0.001$, $^{****}P < 0.0001$. Each group was measured three times.

Discussion

The current investigation reveals that serum-derived exosomes from pediatric patients with severe AD actively promote HaCaT keratinocyte proliferation and secretion of inflammatory mediators, and that these phenotypic changes were primarily driven by the loss of exosomal miR-432-5p, which suppresses its target E2F2 and consequently enhances STAT1 signaling. Furthermore, our clinical data support the utility of exosomal miR-432-5p as a potential non-invasive biomarker for discriminating severe pediatric AD.

A growing body of literature has implicated extracellular vesicles in the pathogenesis of AD [22, 23]. For instance, exosomes obtained from human adipose-derived mesenchymal stem cells have been shown to ameliorate cutaneous inflammation in murine AD models [21]. Neuronal exosomal miRNAs in the serum of AD mice have shown distinct expression patterns compared with those in normal mice [20]. Therefore, EVs are involved in the initiation and propagation of AD. However, research on exosomes from peripheral blood in pediatric AD patients is relatively scarce.

To investigate the molecular mechanisms, we performed miRNA-seq on serum-derived exosomes from AD and healthy controls. Our results showed that both miR-196a-5p and miR-432-5p were significantly downregulated in AD-Exos, as confirmed by RT-qPCR. Among these, miR-432-5p was selected for further study due to its known association with allergic inflammatory states [24]. Prior work has implicated miR-432-5p in the control of cell growth, migratory capacity, and angiogenic processes across diverse tumor types and cardiovascular settings [25-28]. miR-432-5p also regulates vascularization and intra-tumor angiogenesis in osteosarcoma through the miR-432-5p/PDGFB axis. Jin Z et al. showed that miR-432-5p inhibited breast cancer progression by suppressing E2F7 [29, 30]. Few studies have explored the link between miR-432-5p and allergy. Rinku Sharma proposed that circulating miR-432-5p abundance is positively associated with inhaled corticosteroid response in children with asthma, and it may be related to AD [24].

In our study, downregulation of miR-432-5p increased cell proliferation, decreased apoptosis, and enhanced inflammatory cytokine secretion and STAT1 phosphorylation, mimicking the effects of AD-Exos. To further confirm this, we added the miR-432-5p inhibitor to HaCaT cells together with NH-Exos. The results showed increased cell proliferation, elevated pro-inflammatory mediator release, and enhanced STAT1 phosphorylation, which were not statistically different from the AD-Exo group. In summary, these results demonstrate that miR-432-5p downregulation is a key mediator of keratinocyte dysfunction induced by AD serum exosomes.

With respect to the underlying molecular mechanism, we have identified E2F2 as a direct functional target of miR-432-5p. E2F2 belongs to a family of transcription factors that orchestrate cell-cycle progression, differentiation, and programmed cell death by binding to E2F-responsive elements and modulating the transcription of numerous cell-cycle-associated genes [31, 32], and it was selected for further study. Altered Expression of E2F2 is associated with inflammatory diseases. Earlier studies have shown that E2F2 can directly modulate both the STAT1 cascade and the PI3K/AKT/NF-κB pathway, thereby contributing to the pro-inflammatory milieu characteristic of rheumatoid arthritis [33]. Alimujiang A et al. recently investigated the role of apigenin in inhibiting keratinocyte hyperproliferation and inflammation via regulation of the CDK2/E2F2 pathway [34]. In line with these reports, our findings demonstrate that miR-432-5p directly suppresses E2F2 expression, and that the downregulation of miR-432-5p in AD-Exos relieves this suppression, leading to enhanced STAT1 signaling, increased keratinocyte proliferation, and reduced apoptosis. Thus, the miR-432-5p/E2F2/STAT1 axis represents a critical pathway through which AD-derived exosomes promote keratinocyte dysfunction.

Notably, in addition to STAT1-mediated inflammatory and proliferative responses, our study revealed that modulation of the miR-432-5p/E2F2 axis significantly altered p53 expression and apoptosis levels in HaCaT cells. Specifically, restoration of miR-432-5p upregulated p53 and promoted apoptosis, whereas AD-Exos or miR-432-5p inhibition suppressed p53; crucially, E2F2 overexpression reversed the p53 upregulation induced by the miR-432-5p mimic.

Although classically known as an activator of certain pro-apoptotic genes, E2F factors, including E2F2, can also display complex, context-dependent cross-talk with p53. In skin keratinocytes, aberrantly elevated E2F2 may repress p53 expression either through secondary feedback loops (such as MDM2-mediated degradation or repression of p53 co-factors) or by driving hyperproliferation that overrides p53-dependent apoptotic checkpoints [35-38]. By suppressing p53, the loss of exosomal miR-432-5p promotes survival and decreases apoptosis in dysfunctional keratinocytes, contributing to epidermic hyperplasia in AD. Therefore, the miR-432-5p/E2F2 axis bifurcates downstream into the STAT1 pathway (driving proliferation and inflammation) and the p53 pathway (inhibiting apoptosis), jointly driving keratinocyte dysfunction in AD.

This study has several limitations. First, this study enrolled exclusively pediatric patients with severe AD, and the sample size for RNA-seq and ROC analysis is relatively small. Larger cohort studies are needed to validate the diagnostic value of exosomal miR-432-5p. Second, the mechanism of miR-432-5p in other cell types involved in AD pathogenesis, such as immune cells, requires further investigation. Third, the in vivo effects of miR-432-5p modulation have not been explored, and future studies using animal models are warranted. Fourth, while we normalized exosome treatments by total protein concentration-a widely accepted approach in the field-we acknowledge that AD-Exos and NH-Exos may possess distinct specific bioactivities that could theoretically favor different optimal doses. A full dose-response comparison specifically for AD-Exos would provide additional refinement; however, the significant and consistent phenotypic differences observed at the standardized 40 μg/mL dose between the two groups support the validity of our experimental design. Finally, we did not assess the correlation between miR-432-5p/E2F2 levels and clinical factors such as allergen sensitization or comorbidities, which should be addressed in future research.

In conclusion, this study provides the first comprehensive profile of exosomal miRNAs in pediatric patients with severe atopic dermatitis (AD). We demonstrate that AD-derived exosomes carry reduced levels of miR-432-5p, which relieves the suppression of its direct target E2F2, leading to enhanced STAT1 phosphorylation, increased keratinocyte proliferation, and elevated inflammatory responses. Conversely, restoring miR-432-5p expression suppresses these pathological changes. Therefore, the miR-432-5p/E2F2/STAT1 axis represents a potential therapeutic target, and exosomal miR-432-5p may serve as a diagnostic biomarker for severe pediatric AD.

Acknowledgements

This study was supported by Wuxi Municipal Health Commission (No. Z202310).

Disclosure of conflict of interest

None.

Address correspondence to: Ting Yang, Department of Dermatology, Affiliated Children's Hospital of Jiangnan University, No. 299-1 Qingyang Road, Liangxi District, Wuxi 214023, Jiangsu, China. E-mail: 15161515100@163.com

References

[1] Guttman-Yassky E, Simpson E, Esfandiari E, Mano H, Bauer J, Charuworn P and Kabashima K. Rocatinlimab: a novel T-cell rebalancing therapy targeting the OX40 Receptor in atopic dermatitis. Dermatol Ther (Heidelb) 2025; 15: 3153-3171.

[2] Yao Z, Bieber T, Ma L, Wang H, Zhang J, Ni C, Shen J, Li H, Niu H, Shen C, Xiang J, Tang P, Li J, Xu H, Zhang X, Meng C, Luo Y, Li C, Li M, Cheng R, Ran N, Mao X, Mu Z, Xiao F, Ran Q, Zong W, Xu Z, Xu G, Zou X, Han X, Li P, Tang J, Wei F, Liu Q, Zhang H and Guo Y. Phenotypic analysis of atopic dermatitis in children aged 1-12 months: elaboration of novel diagnostic criteria for infants in China and estimation of prevalence. J Eur Acad Dermatol Venereol 2019; 33: 1569-1576.

[3] van der Velde JL, Sprikkelman AB, Vonk JM and Miltner LA. Eczema in early childhood increases the risk of allergic multimorbidity. Clin Transl Allergy 2024; 14: e12384.

[4] Ke H, Yao H and Wei P. Advances in research on gut microbiota and allergic diseases in children. Curr Res Microb Sci 2025; 8: 100362.

[5] Fasseeh AN, Elezbawy B, Korra N, Tannira M, Dalle H, Aderian S, Abaza S and Kaló Z. Burden of atopic dermatitis in adults and adolescents: a systematic literature review. Dermatol Ther (Heidelb) 2022; 12: 2653-2668.

[6] Baidya A and Mabalirajan U. Pathogenesis and management of atopic dermatitis: insights into

epidermal barrier dysfunction and immune mechanisms. Explor Asthma Allergy 2025; 3: 100973.
[7] Wei Y, Gu J, Zhao Z and Gu B. Immunological control of skin development: from homeostasis to developmental pathologies. Front Immunol 2025; 16: 1685633.
[8] Çetinarslan T, Kümper L and Fölster-Holst R. The immunological and structural epidermal barrier dysfunction and skin microbiome in atopic dermatitis-an update. Front Mol Biosci 2023; 10: 1159404.
[9] Zhang C, Qiao P, Xiao C, Cao Z, Chen J, Fang H, Yang J, Kang Z, Dang E, Shao S, Pang B, Li Q, Zhu Z, Shen S, Hasegawa A, Abe R, Qiao H, Wang G and Fu M. Exosomal *miR-375-3p* mediated lipid metabolism, ferritinophagy and CoQ-dependent pathway contributes to the ferroptosis of keratinocyte in SJS/TEN. Int J Biol Sci 2025; 21: 1275-1293.
[10] Wang Y, Xiao T, Zhao C and Li G. The regulation of exosome generation and function in physiological and pathological processes. Int J Mol Sci 2023; 25: 255.
[11] Bayat M and Sadri Nahand J. Exosomal miRNAs: the tumor's trojan horse in selective metastasis. Mol Cancer 2024; 23: 167.
[12] Wang J, Ma W, Si C, Zhang M, Qian W, Park G, Zhou B and Luo D. Exosome-mediated miR-4655-3p contributes to UV radiation-induced bystander effects. Exp Cell Res 2022; 418: 113247.
[13] Weidner J, Bartel S, Kılıç A, Zissler UM, Renz H, Schwarze J, Schmidt-Weber CB, Maes T, Rebane A, Krauss-Etschmann S and Rådinger M. Spotlight on microRNAs in allergy and asthma. Allergy 2021; 76: 1661-1678.
[14] Jakovljevic S, Barjaktarovic I, Jakovljevic D, Levakov O and Vujanovic L. miRNA-146-a, miRNA-21, miRNA-143, miRNA-29-b and miRNA-223 as potential biomarkers for atopic dermatitis. Clin Pract 2025; 15: 192.
[15] Gołuchowska N, Ząber A, Będzichowska A, Tomaszewska A, Rustecka A and Kalicki B. The role of MicroRNA in the pathogenesis of atopic dermatitis. Int J Mol Sci 2025; 26: 5846.
[16] Ljungström M and Oltra E. Methods for extracellular vesicle isolation: relevance for encapsulated miRNAs in disease diagnosis and treatment. Genes (Basel) 2025; 16: 330.
[17] Shah V, Panchal V, Shah A, Vyas B, Bhowmik S, Panchal I and Jain P. Exosomal miRNAs as biomarkers in predicting chemotherapy-induced cardiotoxicity in patients with cancer (Review). Med Int (Lond) 2025; 5: 69.
[18] Chen M, Choi HK, Goldston LL, Hou Y, Jiang C and Lee KB. Advanced cancer liquid biopsy platform for miRNA detection in extracellular vesicles using CRISPR/Cas13a and gold nanoarrays. ACS Nano 2025; 19: 31438-31456.
[19] Shi C, Pei S, Ding Y, Tao C, Zhu Y, Peng Y, Li W and Yi Y. Exosomes with overexpressed miR 147a suppress angiogenesis and infammatory injury in an experimental model of atopic dermatitis. Sci Rep 2023; 13: 8904.
[20] Sung M, Sung SE, Kang KK, Choi JH, Lee S, Kim K, Lim JH, Lee GW, Rim HD, Won S, Kim BS, Kim K, Jang S, Kwak SG, Woo J and Seo MS. Serum-derived neuronal exosomal microRNAs as stress-related biomarkers in an atopic dermatitis model. Biomedicines 2021; 9: 1764.
[21] Mao Y, Xue P, Li L, Xu P, Cai Y, Chu X, Jiang P and Zhu S. Bioinformatics analysis of mRNA and miRNA microarray to identify the key miRNA-gene pairs in small-cell lung cancer. Mol Med Rep 2019; 20: 2199-2208.
[22] Cho BS, Kim JO, Ha DH and Yi YW. Exosomes derived from human adipose tissue-derived mesenchymal stem cells alleviate atopic dermatitis. Stem Cell Res Ther 2018; 9: 187.
[23] Deng T, Zhang Y, Yao Y, Ye P, Zhang D, Cheng F, Wu J, Cheng H and Lu J. Exosome therapeutics: a paradigm shift in skin repair through multidimensional immunomodulation and biomaterial-driven delivery. Biomed Pharmacother 2025; 193: 118830.
[24] Sharma R, Tiwari A, Kho AT, Celedón JC, Weiss ST, Tantisira KG and McGeachie MJ. Systems genomics reveals microRNA regulation of ICS response in childhood asthma. Cells 2023; 12: 1505.
[25] Mohammadinasr M, Montazersaheb S, Molavi O, Kahroba H, Talebi M, Ayromlou H and Hejazi MS. Multiplex analysis of cerebrospinal fluid and serum exosomes MicroRNAs of untreated relapsing remitting multiple sclerosis (RRMS) and proposing noninvasive diagnostic biomarkers. Neuromolecular Med 2023; 25: 402-414.
[26] Xie Z, Liu L, Guo Y, Jiang H, Li L, Qiao Z and Wang J. Exosomal miR-432-5p, miR-4433b-5p, and miR-599: biomarkers for monitoring the severity of Anti-N-methyl-D-aspartate receptor encephalitis. J Integr Neurosci 2025; 24: 37513.
[27] Geng W, Yan S, Li X, Liu Q, Zhang X, Gu X, Tian X and Jiang Y. miR-432-5p inhibits the ferroptosis in cardiomyocytes induced by hypoxia/reoxygenation via Activating Nrf2/SLC7A11 axis by degrading Keap1. Anal Cell Pathol (Amst) 2023; 2023: 1293200.
[28] Chen J, Liu F and Meng X. miR-432-5p targeting SORT1 to protect artery smooth muscle cells and inhibit coronary artery disease. Biochem Genet2025; 63: 5656-5669.
[29] Jin Z, Xu W, Yu K, Luo C, Luo X, Lian T and Liu C. The novel circFKBP8/miR-432-5p/E2F7 cascade functions as a regulatory network in breast cancer. Hereditas 2024; 161: 27.

[30] Wang H, Guo M, Wei H and Chen Y. Targeting p53 pathways: mechanisms, structures, and advances in therapy. Signal Transduct Target Ther 2023; 8: 92.
[31] Li L, Wang S, Zhang Y and Pan J. The E2F transcription factor 2: What do we know? Biosci Trends 2021; 15: 83-92.
[32] Gao Y, Qiao X, Liu Z and Zhang W. The role of E2F2 in cancer progression and its value as a therapeutic target. Front Immunol 2024; 15: 1397303.
[33] Wang S, Wang L, Wu C, Sun S and Pan JH. E2F2 directly regulates the STAT1 and PI3K/AKT/NF-κB pathways to exacerbate the inflammatory phenotype in rheumatoid arthritis synovial fibroblasts and mouse embryonic fibroblasts. Arthritis Res Ther 2018; 20: 225.
[34] Alimujiang A, Kang Y, Wei W, Zhang Z, Bai Y, Zhu Y, Huo S, Xu D and Li Z. Apigenin suppresses keratinocyte hyperproliferation and inflammation in psoriasis by inhibiting CDK2/E2F2 pathway. Phytomedicine 2025; 144: 156486.
[35] Polager S and Ginsberg D. p53 and E2f: partners in life and death. Nat Rev Cancer 2009; 9: 738-748.
[36] Zhou Y, Nakajima R, Shirasawa M, Fikriyanti M, Zhao L, Iwanaga R, Bradford AP, Kurayoshi K, Araki K and Ohtani K. Expanding roles of the E2F-RB-p53 pathway in tumor suppression. Biology (Basel) 2023; 12: 1511.
[37] Li L, Wang S, Zhang Y and Pan J. The E2F transcription factor 2: what do we know? Biosci Trends2021; 15: 83-92.
[38] Iglesias-Ara A, Zenarruzabeitia O, Buelta L, Merino J and Zubiaga AM. E2F1 and E2F2 prevent replicative stress and subsequent p53-dependent organ involution. Cell Death Differ 2015; 22: 1577-1589.